Advances in Nonlinear Variational Inequalities
ISSN: 1092-910X
Vol 27 No. 4 (2024)

MHD Free Convective Heat and Mass Transfer from an Inclined Unsteadily Stretching Plate Embedded in Non-Darcy Porous Media

Dr. Ashok Kumar[1], Dr. M K Sharma[2], Dr. Narender Kumar[3*], Dr. Govil Jindal[4], Seetu Rana[5]

[1,4,5]Assiatant Professor,Department of Mathematics, GGJ Government College, Hisar (Haryana), INDIA

[2]Professor,Department of Mathematics, Guru Jambheshwar University of Science & Technology, Hisar (Haryana), INDIA

[3*]Associate Professor, Department of Physics, Dayanand College, Hisar (Haryana), INDIA

Email:narenderdnc@gmail.com

([*]Corresponding Author)

Article History:

Received: 15-08-2024

Revised: 29-09-2024

Accepted: 08-10-2024

Abstract: An unsteadily stretching inclined plate embedded in a non-Darcy porous medium is considered for the unsteady flow convective heat transfer of electrically conducting viscous incompressible fluid in the presence of static transverse magnetic field. the effect of magnetic field, inclination of the plate and source parameter on the unsteady flow heat and mass transfer through an unsteadily stretching plate embedded in a non-Darcy porous medium. The modeled problem is governed by a set of coupled non-linear differential equations. The coupled first order ordinary differential equations which arise under the given conditions, are solved using Runga-Kutta method. The velocity profiles and temperature profiles for fluid discussed through graphs. The effect of variation of various parameters on velocity and temperature profile are discussed graphically

Keywords: Stretching Plate, Non-Darcy, Porous Media, Runga-Kutta Method, MHD

1. INTRODUCTION

The study of boundary layer flow over a stretching surface is important as it occurs in industry, for example materials manufactured by extrusion, glass fiber and paper production, cooling of metallic plates in a cooling bath etc. In these cases, the final product of desired characteristics depends on the rate of cooling in the process and the process of stretching. By drawing such strip in an electrically conducting fluid subject to magnetic field or through porous media, the rate of cooling can be controlled and final product of desired characteristic might be achieved. Saleh et al. [8] presented the study of convective heat and mass transfer characteristics of an incompressible MHD visco-elastic fluid flow immersed in a porous medium over a stretching sheet with chemical reaction and thermal stratification effects. Changal Raju, et al. [3]investigated the unsteady magnetohydrodinamics flow of an incompressible viscous electrically conducting fluid between two horizontal parallel non-conducting plates, where the lower one is stretching sheet and the upper one is oscillating porous plate, in the presence of a transverse magnetic field and the effects of Hall current. Vidyasagar et al [11]present a study for the steady two-dimensional radiative MHD boundary layer flow of an incompressible, viscous, electrically conducting fluid caused by a non-isothermal linearly stretching sheet placed at the bottom of fluid saturated porous medium. Singh, et al. [10] investigates the MHD boundary layer flow with viscous dissipation and chemical reaction over a stretching porous plate in porous medium. Ghosh et al. [4] investigated the boundary layer flow of a steady incompressible and visco-elastic fluid with short memory (obeying Walters' B fluid model)

passing over a hot vertical porous plate in the presence of transverse magnetic field. Barik et al [1] studied the heat and mass transfer effect on the flow over a stretching sheet in the presence of a heat source and considered the span wise variation of magnetic field strength, heat source and heat flux and also considered the effect of viscous dissipation. Yohannws et al[13]investigated the convective heat and mass transfer in nanofluid flowthrough a porous media due to a stretching sheet subjected to magnetic field, viscous dissipation, chemical reaction and Soret effects. Singh et al. [9] focused their investigation to developed a mathematical model and comparative study of combined effects of free convective heat and mass transfer on the steady two - dimensional, laminar fluid flow past a moving permeable vertical surface in a porous medium subject to a transverse uniform magnetic field. Bhukta et al. [2]studied the heat and mass transfer effect in a boundary layer flow through porous medium of an electrically conducting viscoelastic fluid over a shrinking sheet subject to transverse magnetic field in the presence of heat source. Rashidi et al. [8] applied the homotopy analysis method is employed to examine free convective heat and mass transfer in a steady two-dimensional magnetohydrodynamic fluid flow over a stretching vertical surface in porous medium. Hunegnaw, D. et al. [5] analyzed MHD boundary layer flow and heat transfer of a fluid with variable viscosity through a porous medium towards a stretching sheet by taking in to the effects of viscous dissipation in presence of heat source/sink. Prakash et al [6] developed a numerical model to study hydromagnetic unsteady laminar boundary layer flow of viscous, incompressible fluid over a vertical stretching plate embedded in a sparsely packed porous medium in the presence of non-uniform heat generation/absorption. Yadav et al [12] investigated radiation effects on the MHD flow over an exponentially moving stretching sheet placed in a porous medium with variable magnetic field which is applied normal to the sheet. The aim of the present study is to analyze the effect of magnetic field, inclination of the plate and source parameter on the unsteady flow heat and mass transfer in non-Darcy porous medium.

2. FORMULATION OF THE PROBLEM

A semi-infinite plate which is inclined at an angle α from the vertical is embedded in a non-Darcy porous media with saturated viscous incompressible electrically conducting fluid. The origin of the system is located at the slit from which the plate is drawn. The x-axis is taken along the continuous stretching surface and points in the direction of motion. The y–axis is perpendicular of the plate. The plate is subjected to unsteady stretching. The temperature of the plate and mass concentration at the plate are also unsteady while the ambient temperature T_∞ and ambient concentration C_∞ are taken to be constant and very small in magnitude. The problem is modeled to analyze the MHD flow, heat and mass transfer through the inclined plate in the influence of a static magnetic field of strength $(0,B_0,0)$ normal to the plate and a heat source of strength Q_0. For viscous incompressible fluid the equation of continuity is

$$\frac{\partial u}{\partial x}+\frac{\partial v}{\partial y}=0 \quad (1)$$

The equation of motion under usual Boussinesq's approximation is given by

$$\frac{\partial u}{\partial t}+u\frac{\partial u}{\partial x}+v\frac{\partial u}{\partial y}=\upsilon\frac{\partial^2 u}{\partial y^2}-\frac{\upsilon}{K}u-\frac{\sigma {B_0}^2 u}{\rho}-\frac{C_d}{\sqrt{K}}u^2+g\beta\left(T-T_\infty\right)\cos\alpha+g\beta^*\left(C-C_\infty\right)\cos\alpha$$

(2)

The equation of energy

$$\rho C_p\left(\frac{\partial T}{\partial t}+u\frac{\partial T}{\partial x}+v\frac{\partial T}{\partial y}\right)=\kappa\frac{\partial^2 T}{\partial y^2}+Q_0\left(T-T_\infty\right) \qquad (3)$$

The mass diffusion equation

$$\frac{\partial C}{\partial t}+u\frac{\partial C}{\partial x}+v\frac{\partial C}{\partial y}=D\frac{\partial^2 C}{\partial y^2} \qquad (4)$$

it is assumed that the viscous dissipation is negligible.

where, u and v are velocity components in the x, y-directions, respectively $\upsilon=\mu/\rho$ the kinematic viscosity, μ the coefficient of viscosity, ρ the density of the fluid, σ the electrical conductivity of the fluid, T the fluid temperature , κ the thermal conductivity, C_p the specific heat at constant pressure,Q_0 the heat source strength, C_d the drag coefficient, K the permeability of the medium, β the coefficient of volumetric thermal expansion, β^* the coefficient of volumetric concentration expansion, D mass diffusivity coefficient.The boundary conditions associated with the problem are

$$y=0:\ u=U_w,\quad v=0,\quad T=T_w,\ C=C_w$$

$$y\to\infty:\ u=0,\quad T=T_\infty,\quad C=C_\infty \qquad (5)$$

were,

$$U_w(x,t)=\frac{ax}{1-\gamma t},\ T_w(x,t)=\frac{bx}{1-\gamma t},\ C_w(x,t)=\frac{c\,x}{1-\gamma t}$$

a , b, c and γ are constants.

3. METHOD OF SOLUTION

To solve the coupled non-linear partial differential equations (2) to (4) introducing following similarity transformation

$$\eta=y\sqrt{\frac{U_w}{\upsilon x}}$$

$$\psi=\sqrt{\nu x U_w}\,f(\eta)$$

$$\theta(\eta)=\frac{T-T_\infty}{T_w-T_\infty}$$

$$\phi(\eta)=\frac{C-C_\infty}{C_w-C_\infty} \qquad (6)$$

With this transformation if u and v are considered as $u=\frac{\partial\psi}{\partial y}$ $v=-\frac{\partial\psi}{\partial x}$ then the equation of continuity is identically satisfied.

Then the expression for u, v, T, C and their derivatives involved in the equation (2) to (4) are known in the form of $f(\eta),\ \theta(\eta),\ \phi(\eta)$ and are given below

$$u=\frac{\partial\psi}{\partial\eta}\frac{\partial\eta}{\partial y}=\sqrt{\nu x U_w}f'(\eta)\sqrt{\frac{U_w}{\nu x}}=U_w f'(\eta),\ v=-\upsilon\sqrt{\frac{U_w}{\upsilon x}}f(\eta)$$

$$\frac{\partial u}{\partial y}=U_w f''(\eta)\frac{\partial\eta}{\partial y}=U_w f''(\eta)\sqrt{\frac{a}{\nu}}\frac{1}{\sqrt{1-\gamma t}}$$

$$\frac{\partial u}{\partial x}=\frac{a}{1-\gamma t}f'(\eta),\ \frac{\partial^2 u}{\partial y^2}=U_w\frac{a}{\nu(1-\gamma t)}f'''(\eta),\ \frac{\partial u}{\partial t}=U_w\frac{\gamma}{1-\gamma t}\left(f'(\eta)+\frac{\eta}{2}f''(\eta)\right)$$

$$\frac{\partial T}{\partial t}=T_w\frac{\gamma}{1-\gamma t}\theta(\eta)+(T_w-T_\infty)\frac{\gamma}{1-\gamma t}\frac{\eta}{2}\theta'(\eta)$$

$$\frac{\partial T}{\partial x}=\frac{T_w}{x}\theta(\eta),\ \frac{\partial T}{\partial y}=(T_w-T_\infty)\theta'(\eta)\sqrt{\frac{U_w}{\upsilon x}},\ \frac{\partial^2 T}{\partial y^2}=(T_w-T_\infty)\theta''(\eta)\frac{U_w}{\upsilon x}$$

$$\frac{\partial C}{\partial t}=C_w\frac{\gamma}{1-\gamma t}\phi(\eta)+(C_w-C_\infty)\frac{\gamma}{1-\gamma t}\frac{\eta}{2}\phi'(\eta)$$

$$\frac{\partial C}{\partial x}=\frac{C_w}{x}\phi(\eta),\ \frac{\partial C}{\partial y}=(C_w-C_\infty)\phi'(\eta)\sqrt{\frac{U_w}{\upsilon x}},\ \frac{\partial^2 C}{\partial y^2}=(C_w-C_\infty)\phi''(\eta)\frac{U_w}{\upsilon x}$$

where, primes denote the differentiation with respect to η.

Incorporating above expression in (2) to (4) the reduced equation of motion, energy and diffusion are ordinary differential equations given by

$$A\left(f'+\frac{\eta}{2}f''\right)+f'^2-ff''=f'''-\lambda f'-Mf'+G_r\theta\cos\alpha+G_m\phi\cos\alpha-\hat{F}(f')^2 \qquad (7)$$

$$A\left(\theta+\frac{\eta}{2}\theta'\right)+(f'\theta-f\theta')+\lambda(A\theta+f'\theta)=\frac{1}{\Pr}\theta''+Q\theta \qquad (8)$$

$$A\left(\phi+\frac{\eta}{2}\phi'\right)+(f'\phi-f\phi')+\lambda'(A\phi+f'\phi)=\frac{1}{Sc}\theta'' \qquad (9)$$

where, $A=\frac{\gamma}{a}$ is the unsteadiness parameter, $G_r=\frac{g\beta(T_w-T_\infty)x}{U_w{}^2}$ the local temperature Grashof number, $G_m=\frac{g\beta^*(C_w-C_\infty)x}{U_w{}^2}$ the local mass Grashof number, $\Pr=\frac{\mu C_p}{\kappa}$ the Prandtl number, $\hat{F}=\frac{C_d x}{\sqrt{K}}$ the non-Darcy parameter, $Q=\frac{Q_0 x}{\rho C_p U_w}$ the heat source parameter, $\lambda=\frac{T_\infty}{T_w-T_\infty}<<1$ and $\lambda'=\frac{C_\infty}{C_w-C_\infty}<<1$ since T_∞ and C_∞ is infinitesimal

The corresponding boundary conditions are

$$\eta=0:\ f'(\eta)=1,\quad f(\eta)=0,\quad \theta(\eta)=1,,\ \phi(\eta)=1$$

$$\eta\to\infty:\ f'(\eta)=0,\quad \theta(\eta)=0,\ \phi(\eta)=0 \qquad (10)$$

3. Numerical Solution

The equations (7) to (9) are non-linear ordinary coupled differential equations. For the solution these equations Runge-Kutta (4th order) method was adopted. To implement Runga-Kutta method, the higher order differential equations (7) and (9) are converted into a set of first order differential equations by taking as $F_0 = f(\eta)$, $\theta_0 = \theta(\eta)$ and $\phi_0 = \phi(\eta)$ as follows

$$F_1 = \frac{dF_0}{d\eta} \qquad (11)$$

$$F_2 = \frac{dF_0}{d\eta} \qquad (12)$$

$$\theta_1 = \frac{d\theta_0}{d\eta} \qquad (13)$$

$$\phi_1 = \frac{d\phi_0}{d\eta} \qquad (14)$$

$$\frac{dF_2}{d\eta} = A(F_1 + \frac{\eta}{2}F_2) + F_1^2 - F_0F_2 + \lambda F_1 + MF_1 - G_r\theta_0\cos\alpha - G_m\phi_0\cos\alpha + \hat{F}F_1^2 \qquad (15)$$

$$\frac{d\theta_1}{d\eta} = A\,\mathrm{Pr}(\theta_0 + \frac{\eta}{2}\theta_1) + \mathrm{Pr}(F_1\theta_0 - F_0\theta_1) + \lambda\,\mathrm{Pr}(A + F_1)\theta_0 - \mathrm{Pr}\,Q \qquad (16)$$

$$\frac{d\phi_1}{d\eta} = ASc(\phi_0 + \frac{\eta}{2}\phi_1) + Sc(F_1\phi_0 - F_0\phi_1) + \lambda' Sc(A + F_1)\phi_0 \qquad (17)$$

Along with the boundary conditions

$$F_0(0) = 0,\quad F_1(0) = 1, \theta_0(0) = 1,\ \phi_0(0) = 1$$

$$F_1(\infty) = 0,\ \theta_0(\infty) = 0,\ \phi_0(\infty) = 0 \qquad (18)$$

Now the equations from (11) to (17) are seven coupled first order ordinary differential equations whose solution is to be obtained with Runga-Kutta method. For the proper implementation of Runga-Kutta method the seven initial conditions namely $F_0(0), F_1(0), F_2(0), \theta_0(0), \theta_1(0), \phi_0(0)$ and $\phi_1(0)$ are required. But $F_2(0), \theta_1(0)$ and $\phi_1(0)$ are not known, therefore they must be first guessed properly and refined to approximate the boundary condition. The Newton's iterative method on a system of non-linear equations for iteratively refining x, by a correction h

$$x_{i+1} = x_i + h \qquad (19)$$

where, h is calculated by linear extrapolation of f(x) to zero, that is

$$f(x_i) + h\left(\frac{df}{dx_i}\right)_{x_i} = 0 \qquad (20)$$

is used to approximate the value of $F_2(0), \theta_1(0)$ and $\phi_1(0)$. In the present problem, the equations in matrix form are

$$\underline{X}_{i+1} = \underline{X}_i + \underline{H} \tag{21}$$

and

$$\underline{F} + \underline{\underline{K}}\,\underline{H} = 0 \tag{22}$$

where,

$$\underline{X}_{i+1} = \begin{bmatrix} F_2(\eta=0)_{i+1} \\ \theta_1(\eta=0)_{i+1} \\ \phi_1(\eta=0)_{i+1} \end{bmatrix},\ \underline{X}_i = \begin{bmatrix} F_2(\eta=0)_i \\ \theta_1(\eta=0)_i \\ \phi_1(\eta=0)_i \end{bmatrix},$$

$\underline{H}_{i+1} = \begin{bmatrix} dF_2 \\ d\theta_1 \\ d\phi_1 \end{bmatrix}$ is matrix of stepsize

$$\underline{F} = \begin{bmatrix} F_2(\eta_{\max})_i \\ \theta_1(\eta_{\max})_i \\ \phi_1(\eta_{\max})_i \end{bmatrix}$$

and $\underline{\underline{K}}$ is the Jacobian matrix defined as

$$\underline{\underline{K}} = \frac{\partial(F_1(\eta_{\max}), \theta_0(\eta_{\max}), \phi_0(\eta_{\max}))}{\partial(F_2(\eta=0), \theta_0(\eta=0), \phi_0(\eta=0))}$$

The component $K(1,1) = \left.\dfrac{dF_1(\eta_{\max})}{dF_2(\eta=0)}\right|_{(\theta_1,\phi_1)} = \dfrac{F_1(\eta_{\max})\big|_{F_2+\delta F} - F_1(\eta_{\max})\big|_{F_2}}{\delta F}$

For the estimation nine derivatives, the ordinary differential equations (11) to (17) are solved with four pairs of initial values $\{\partial((F_2)_i, (\theta_1)_i, (\phi_1)_i)\}$, $\{\partial((F_2)_i + \delta_F, (\theta_1)_i, (\phi_1)_i)\}$, $\{\partial((F_2)_i, (\theta_1)_i + \delta_\theta, (\phi_1)_i)\}$, $\{\partial((F_2)_i, (\theta_1)_i, (\phi_1)_i + \delta_\phi)\}$ where $\delta_F = dF_2 = 0.005$, $\delta_\theta = d\theta_1 = 0.005$ $\delta_\phi = d\phi_1 = 0.005$, with a tolerance of order 10^{-7}.

4. RESULT AND DISUSSION

The numerical values of non-dimensional quantities velocity $f'(\eta)$, temperature $\theta(\eta)$ and concentration $\phi(\eta)$ are computed and corresponding figures are plotted with Matlab for three sets of various physical parameters involved in the problem. Figure 7.2 shows the effect of magnetic field on $f'(\eta)$. From the figure it ii observed that with the increase in magnetic parameter that is magnetic field strength, the flow velocity is retarded significantly as a consequence of Lorenzian force. The results are in good agreement with the physical phenomenon of Lorenzian force. In figure 7.3, the effect of modified Grashof number Gm on the flow profile $f'(\eta)$ are plotted and observed that the value of $f'(\eta)$ decreases with increase in Gm. For small value of Gm, the value of $f'(\eta)$ near the plate is greater than the

boundary value at the plate shows the momentum gain that imparted by the stretching of the plate. But with the increase of Gm the value of $f'(\eta)$ decreases significantly and reverse flow seen for Gm>5. Figure 7.4 depicts the effect of Grashof number Gr on $f'(\eta)$. The value of $f'(\eta)$ decreases in small magnitude with increase in Gr. Figure 7.5 demonstrates the variation in $f'(\eta)$ with the value Prandtl number. The value of $f'(\eta)$ for Pr=0.72 is significantly high as compare to when Pr=7.0 and other value greater to it. The effect of non-Darcy parameter on the flow profile $f'(\eta)$ as shown in figure 7.6 describes that if the value of non-Darcy parameter is increasing the flow is slowed down as a result of increase in solid-fluid interaction drag force. From figure 7.7 it is plausible that the inclination in the plate from vertical retarded fluid velocity in a magnificent way. When α=0 that is plate is vertical then in the vicinity of the plate a significant effect of stretching plate on the fluid velocity is observed as compare to that when plate is inclined. Figure 7.8 shows that near to the plate $f'(\eta)$ increases with the increase in unsteadiness parameter while away from the plate there is slight oscillation in $f'(\eta)$ with respect to increase in parameter A. Figure 7.9 demonstrates that the effect of heat source parameter on $f'(\eta)$. The increase in source parameter increases fluid velocity as a consequence of enhanced momentum advection in the fluid. It is good in agreement with the results of physical phenomenon. The flow profile $f'(\eta)$ decreases with the increase in Schmidt number is clear from the figure 7.10. From figure 7.11 it is observed that the fluid temperature increases with the increase in magnetic number M. As similar to the velocity profile the temperature also decreases with increase in the modified Grashof number Gm and Grashof number Gr as seen in the figures 7.12 and 7.13 respectively. Figure 7.14 shows that with the increase in Prandtl number, the temperature of the fluid increases as a result of higher momentum diffusivity of the fluid. In contrast to the velocity profile , the temperature of the fluid increases with the increase in non-Darcy parameter F, but the effects are in less profound as observed from Figure 7.15. The figure 7.16 shows fluid temperature is higher when the plate inclination from the vertical increases, means the convection of heat in case of vertical plate is more due to maximum buoyancy force which is reduced by the factor ($g\cos\alpha$) in case of inclination is increased. In figure 7.17 it is observed that temperature of the fluid at lower value of unsteady parameter A is higher compare to at that of higher value. At the same it is clear from the figure that this parameter affects in a small magnitude. Figure 7.18 describe that with the increase in heat source strength the temperature of the fluid rises profoundly and a positive gradient present closer to the plate at high value of Q. it is seen from the figure 7.19 that increase in Schmidt number contribute in the rise of the fluid temperature. Similar to the temperature profile the concentration profile also increases with the increase in magnetic field strength as observed in figure 7.20. Figure 7.21 demonstrate that contrast to the velocity and temperature profile the concentration profile are enhanced with the increase in modified Grashof number Gm. The effects of Gr, Pr, F, A and Q on the concentration profile are not so profound as compare to the velocity and temperature profiles at the same values, are plausible from figure 7.22, 7.23,7.24 and 7.26 respectively. Figure 7.25 demonstrates that the concentration of the fluid remains at higher level when the inclination from the vertical increases that caused by the term $g\cos\alpha$. The increase in Schmidt number brings down the fluid concentration is observed in the figure7.28.

5. CONCLUSIONS

- Increase in magnetic parameter that is magnetic field strength, the flow velocity is retarded significantly and fluid temperature increases which are in good agreement with the physical phenomenon of Lorezian force.
- The increase in Gm adversely affect on the flow velocity and temperature of the fluid

- The value of $f'(\eta)$ for Pr=0.72 is significantly high as compare to when Pr=7.0 and other value greater to 0.72
- Increase in non-Darcy parameter slowed down the fluid velocity that correlate the increase in solid-fluid interaction drag force.
- The inclination in the plate from vertical retarded the fluid velocity in a magnificent way.At the same time fluid temperature increases which is caused by presence of the factor($g\cos\alpha$)
- The concentration of the fluid remains at higher level when the inclination from the vertical increased, caused by the term $g\cos\alpha$.

REFRENCES

[1] Barik R.N. Dash, G.C.and Rath, P.K. (2012) "Heat and mass transfer on MHD flow through a porous medium over a stretching surface with heat source." Mathematical Theory and Modeling, Vol. 2(7) ISSN 2224-5804.

[2] Bhukta, D., Dash, G.C. and Mishra, S.R. (2014) "Heat and mass transfer on mhd flow of a viscoelastic fluid through porous media over a shrinking sheet." International Scholarly Research Notices,Vol.2014 (2014), Article ID 572162, 11 pages.

[3] Changal Raju, M., Raddy, N. A. and Sibyala, V. K. V. (2011) "Hall-current effects on unsteady magnetohydrodinamics flow between stretching sheet and an oscillating porous upper parallel plate with constant suction." THERMAL SCIENCE, Vol. 15(2), pp. 527-536.

[4] Ghosh, S. and Shit, G.(2012) "Mixed Convection MHD Flow of Viscoelastic Fluid in a Porous Medium past a Hot Vertical Plate," World Journal of Mechanics, vol. 2 (5), pp. 262-271.

[5] Hunegnaw, D. and Naikoti, K. (2014) "MHD effects on heat transfer over stretching sheet embedded in porous medium with variable viscosity, viscous dissipation and heat source/sink." Ain Shams Engineering Journal, vol. 5(3),pp.967-977.

[6] Prakash , D., Muthtamilselvan, M. and Doh D. H. (2014) Unsteady MHD non-Darcian flow over a vertical stretching plate embedded in a porous medium with non-uniform heat generation. Applied Mathematics and computation, 06/2014; 236:480–492. DOI: 10.1016/j.amc.2014.03.072

[7] Rashidi M.M, Rostami, B., Freidoonimehr, N. and Abbasbandy, S.(2014) "Free convective heat and mass transfer for MHD fluid flow over a permeable vertical stretching sheet in the presence of the radiation and buoyancy effects." Ain Shams Engineering Journal, vol. 5(3),pp.901-912.

[8] Saleh, M.A, Mohamed, A.A.B and Mahmoud, S.E.G(2010) "Heat and mass transfer in mhdvisco-elastic fluid flow through a porous medium over a stretching sheet with chemical reaction."

[9] Singh, A K. and Madhab, B.(2013) "MHD Free Convective Heat and Mass transfer of fluid flow past a moving variable surface in porous media". International Journal of Engineering Trends and Technology 4(4), 1151-1157.

[10] Singh, P.K. and Singh, J. (2012) "MHD Flow with Viscous Dissipation and Chemical Reaction over a Stretching Porous Plate in Porous Medium." International Journal of Engineering Research and Applications, Vol. 2(2) pp. 1556-1564.

[11] Vidyasagar, G., Reddi,B. A.P., Ramana, B. and Sugunamma, V.(2012) "Mass transfer effects on radiative MHD flow over a non isothermal stretching sheet embedded in a porous medium."

[12] Yadav, R.S. and Sharma, P.R (2014)"Effects of radiation and viscous dissipation on MHD boundary layer flow due to an exponentially moving stretching sheet in porous medium." Asian Journal of Multidisciplinary Studies, Vol. 2(8) ISSN:2321.
[13] Yohannes, K.Y. and Shankar B.(2013) "Heat and mass transfer in MHD flow of nanofluids through aporous media due to a stretching sheet with viscous dissipationand chemical reaction effects.", Carib.J.SciTech, 1(1),1-17.

6. FIGURES

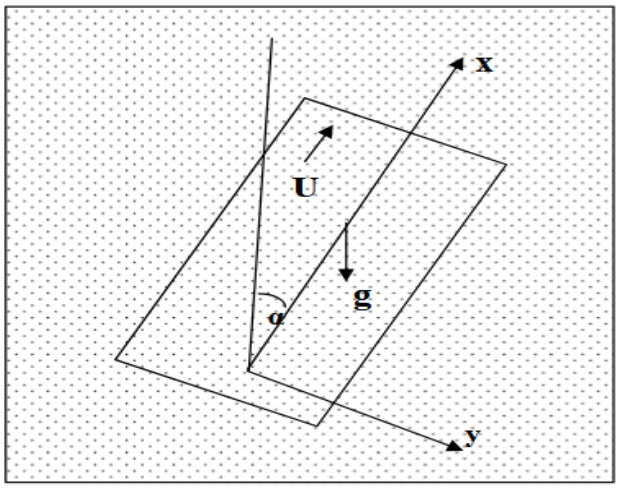

Figure 7.1 Physical model of the problem

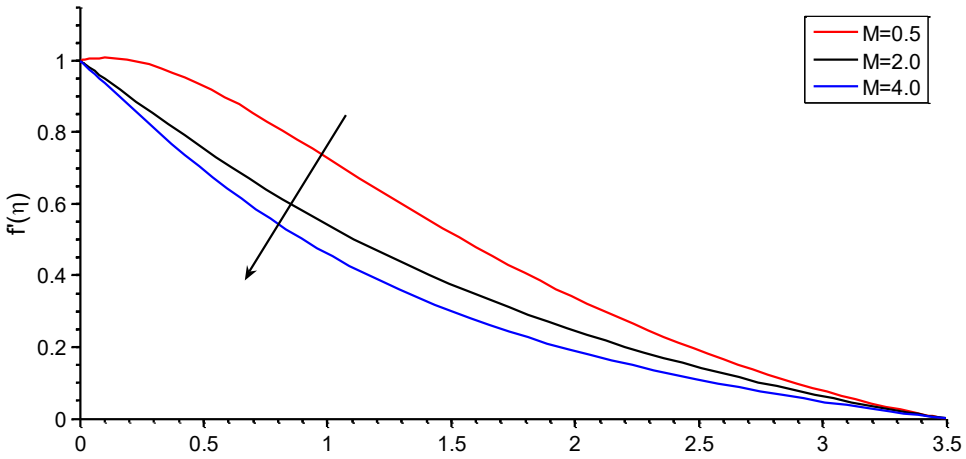

Figure7.2 Variation of fluid flow profile with the Hartmann number
λ=0.001, α=π/3,A=0.25,Gr=5, F=0.1, Gm=5, Pr=1.5, Q=0.2, Sc=0.2

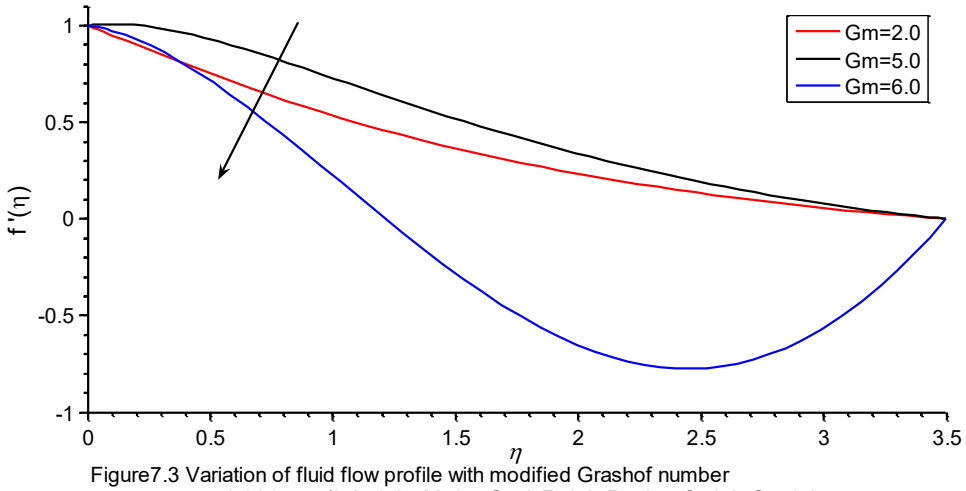

Figure7.3 Variation of fluid flow profile with modified Grashof number
λ=0.001, α=π/3,A=0.25,M=0.5,Gr=2,F=0.2, Pr=1.5, Q=0.2, Sc=0.2

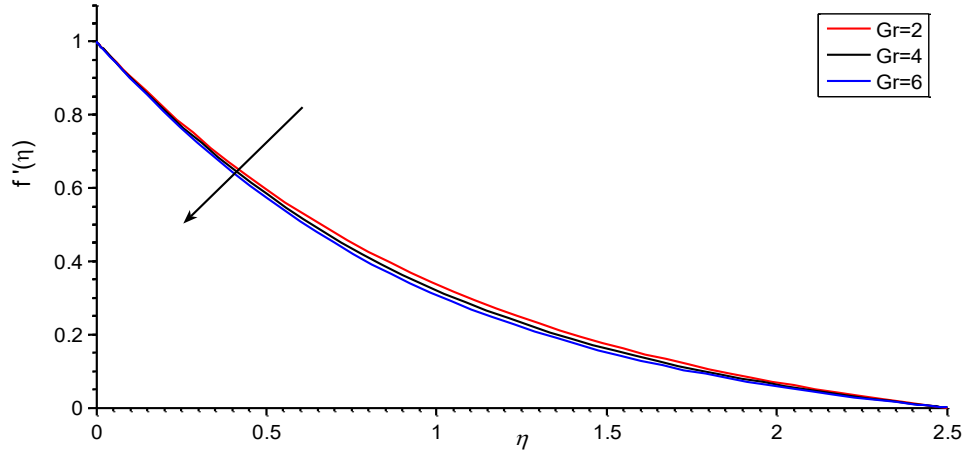

Figure7.4 Variation of fluid flow profile with the Grashof number
λ=0.001, α=π/3,A=0.25,M=0.5, F=0.1, Gm=5, Pr=1.5, Q=0.2, Sc=0.2

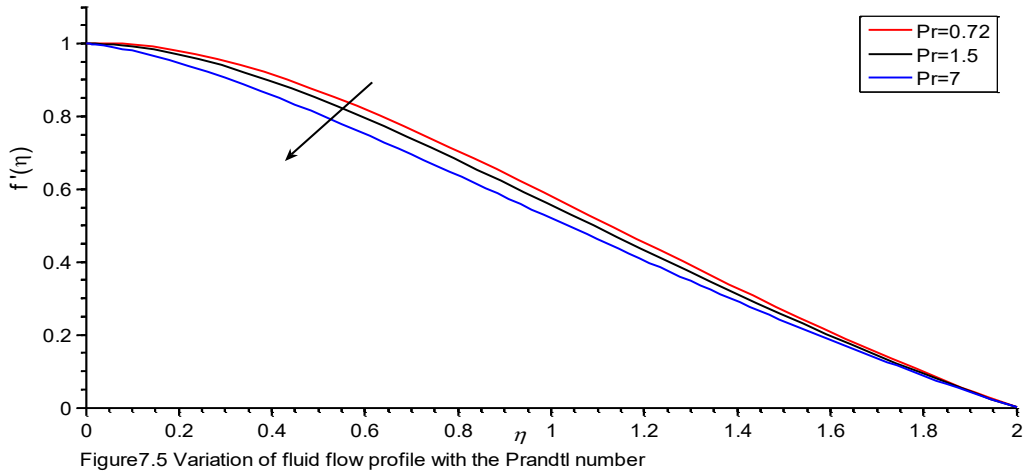

Figure7.5 Variation of fluid flow profile with the Prandtl number
λ=0.001, α=π/3,A=0.25,Gr=5, F=0.1, Gm=5, M=0.5, Q=0.2, Sc=0.2

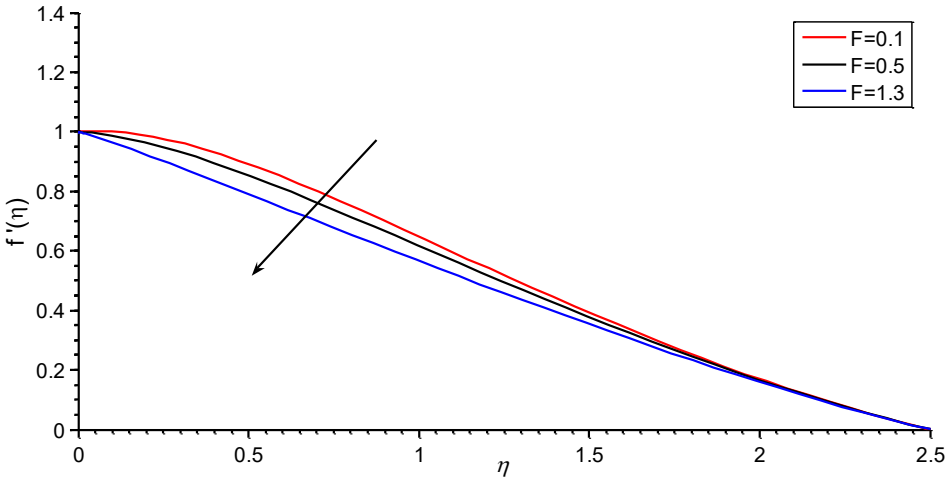

Figure7.6 Variation of fluid flow profile with the non Darcy parameter
λ=0.001, α=π/3,A=0.25,M=0.5,Gr=2, Gm=5, Pr=1.5, Q=0.2, Sc=0

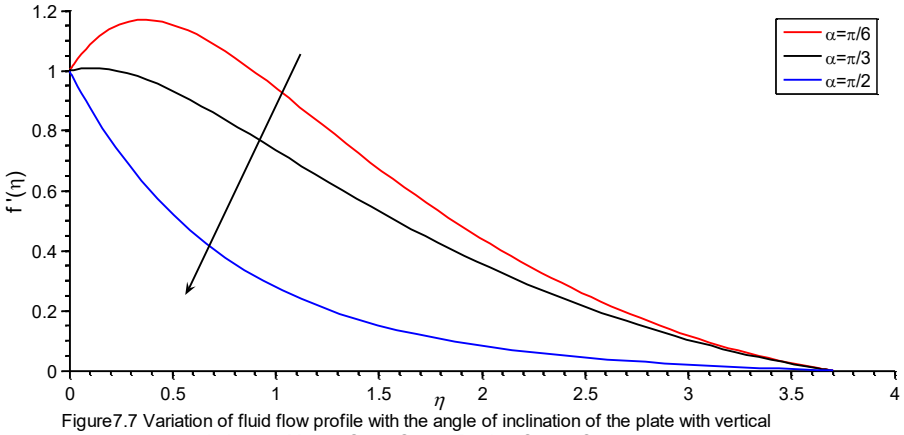

Figure7.7 Variation of fluid flow profile with the angle of inclination of the plate with vertical
λ=0.001, A=0.25,M=0.5, Gr=2, Gm=5, Pr=1.5, Q=0.2, Sc=0.2

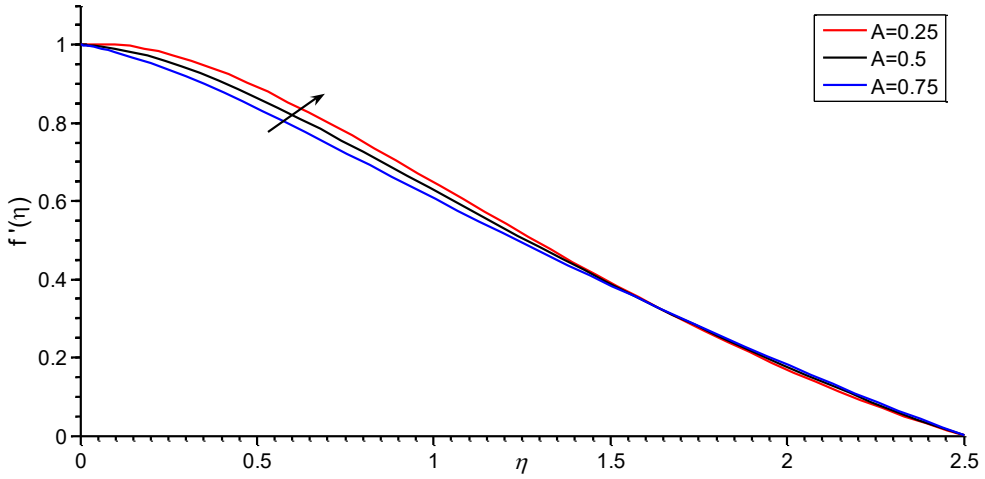

Figure7.8 Variation of fluid flow profile with the usteady parameter
λ=0.001, α=π/3,M=0.5, F=0.1,Gr=2, Gm=5, Pr=1.5, Q=0.2, Sc=0.2

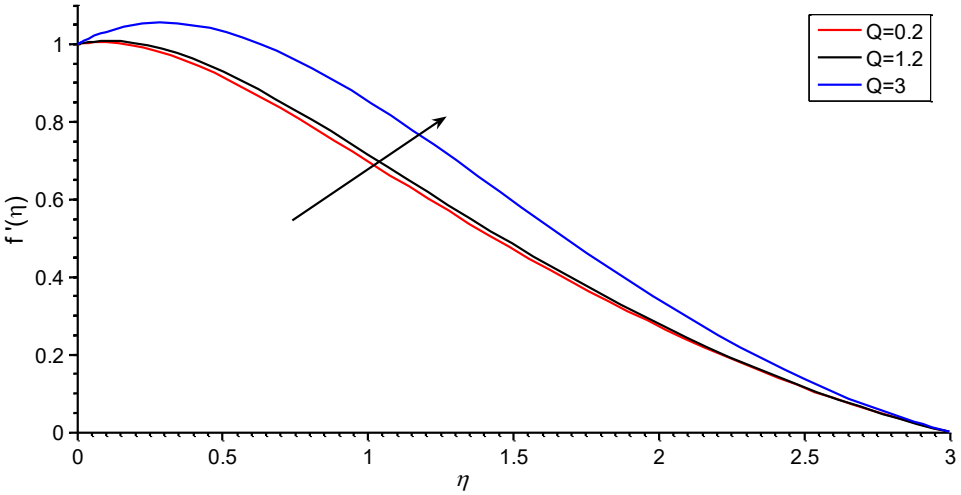

Figure7.9 Variation of fluid flow profile with heat source parameter
λ=0.001, α=π/3,A=0.25,Gr=5, F=0.1, Gm=5, M=0.5, Pr=1.5, Sc=0.2

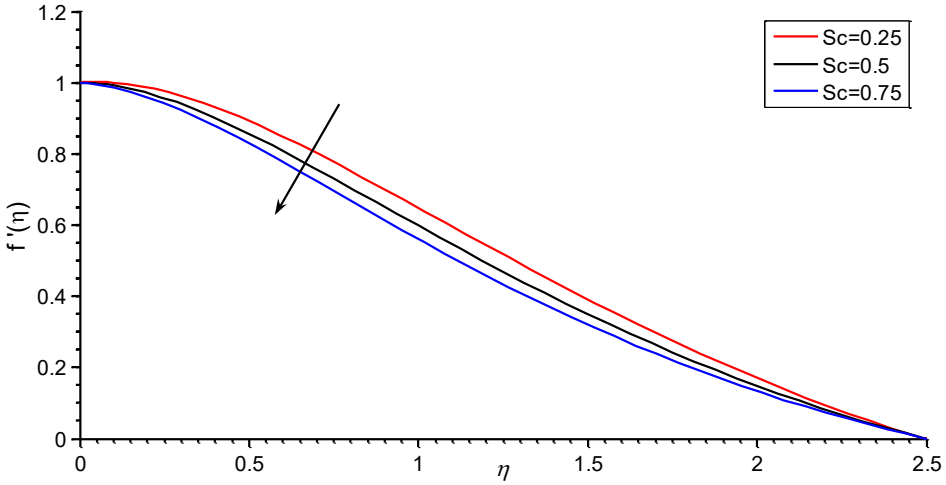

Figure7.10 Variation of fluid flow profile with Schmidt number at
A=0.25, α = π/3, λ=0.001,Gr=2,Gm=5,F=0.1,M=0.5,Pr=1.5,Q=0.2

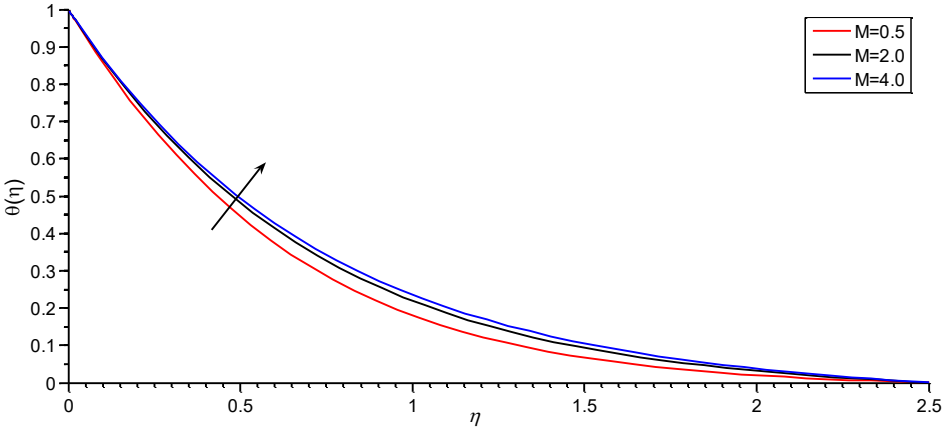

Figure7.11 Variation of temmperature of fluid with the Hartmann number number
λ=0.001, α=π/3,A=0.25,Gr=5, F=0.1, Gm=5, Pr=1.5, Q=0.2, Sc=0.2

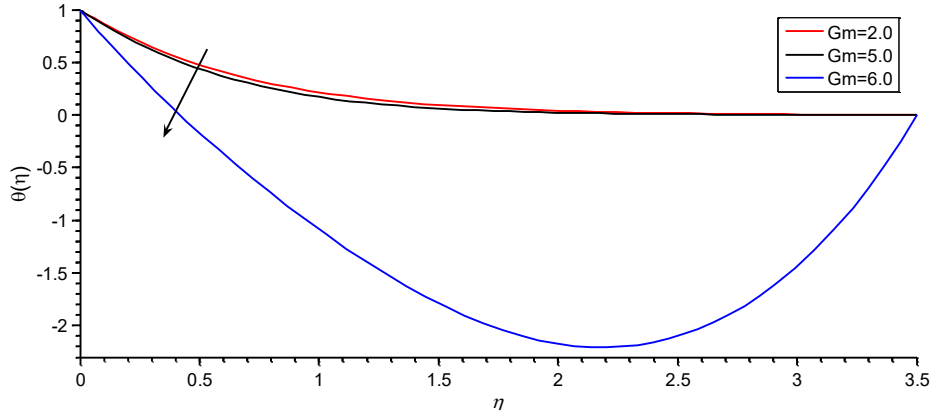

Figure7.12 Variation of temperature of fluid with the modified Grashof number
λ=0.001, α=π/3,A=0.25,M=0.5,Gr=2,F=0.1 Pr=1.5, Q=0.2, Sc=0.2

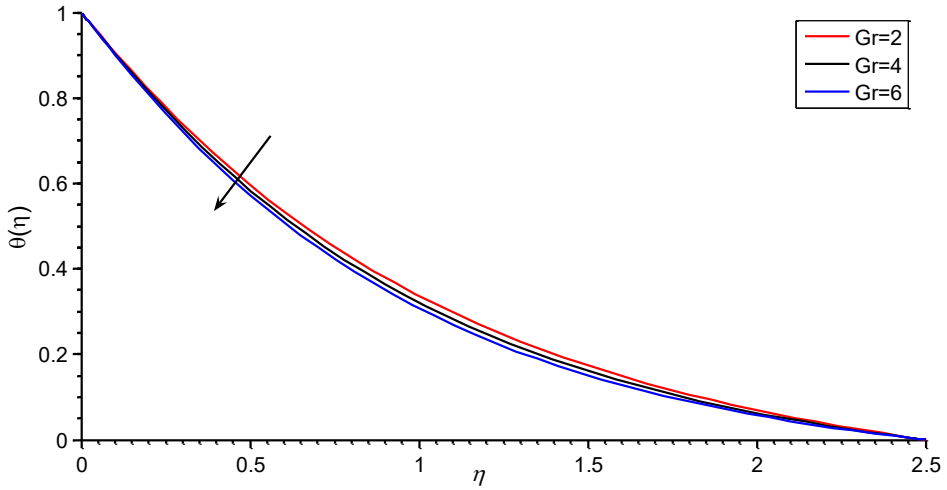

Figure7.13 Variation of temperature of fluid with the Grashof number
λ=0.001, α=π/3,A=0.25,M=0.5, F=0.1, Gm=5, Pr=1.5, Q=0.2, Sc=0.2

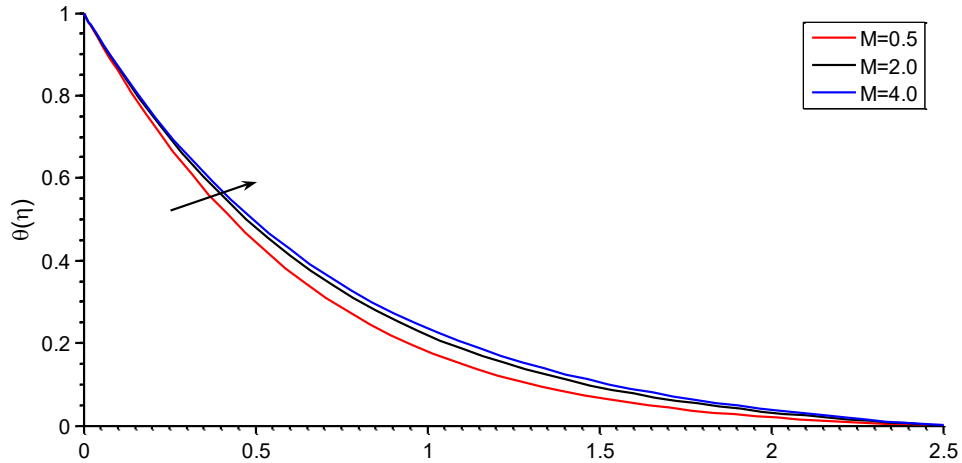

Figure7.14 Variation of temperature with the Prandtl number
λ=0.001, α=π/3,A=0.25,Gr=5, F=0.1, Gm=5, M=0.5, Q=0.2, Sc=0.2

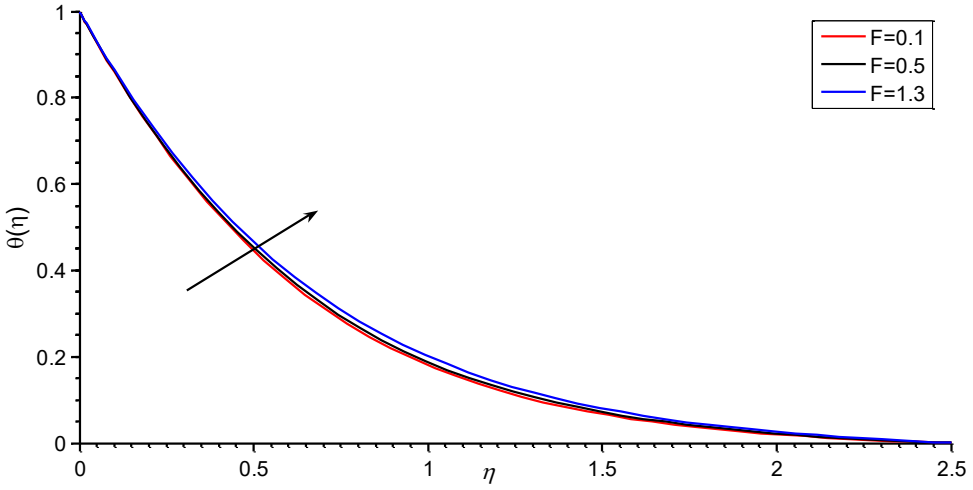

Figure7.15 Variation of temperature of fluid with the non Darcy parameter
λ=0.001, α=π/3,A=0.25,M=0.5,Gr=2, Gm=5, Pr=1.5, Q=0.2, Sc=0.2

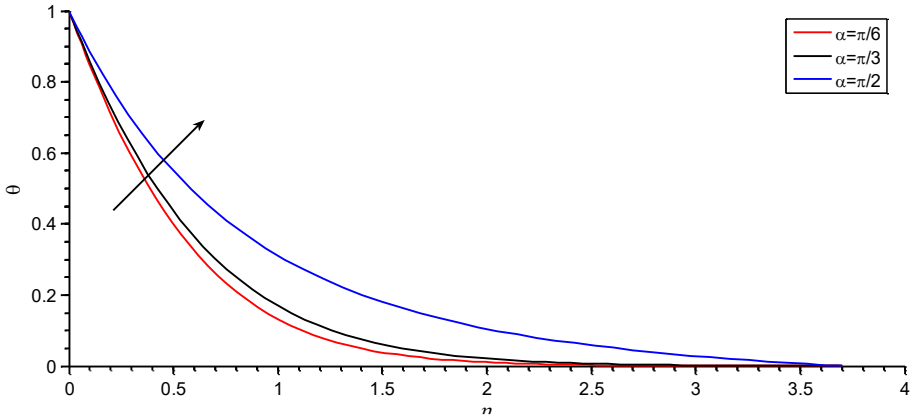

Figure7.16 Variation of temperature of fluid with the angle of inclination of the plate with vertical
λ=0.001, A=0.25,M=0.5, Gr=2, Gm=5, Pr=1.5, Q=0.2, Sc=0.2

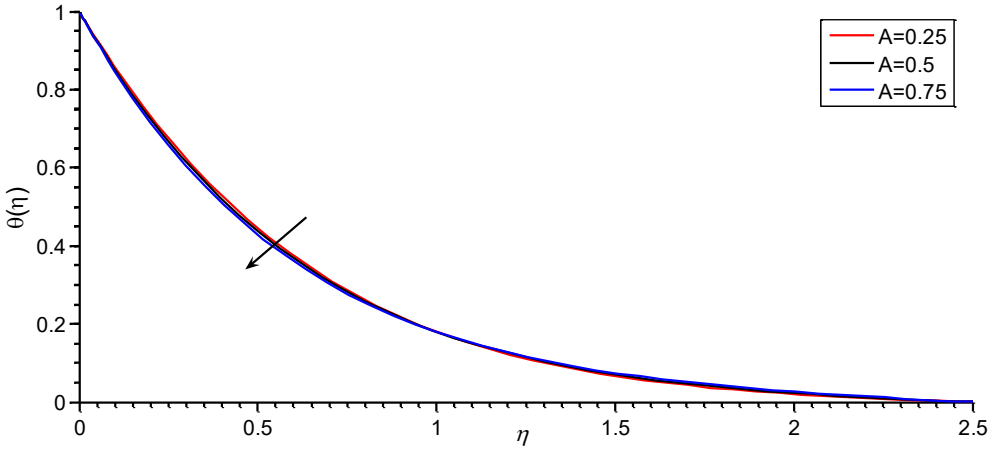

Figure7.17 Variation of temperature of fluid with the usteady parameter
λ=0.001, α=π/3,M=0.5, F=0.1,Gr=2, Gm=5, Pr=1.5, Q=0.2, Sc=0.2

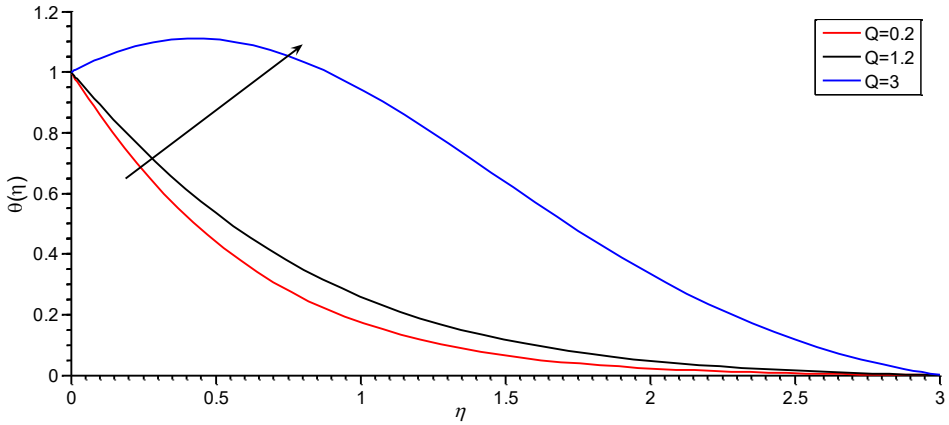

Figure7.18 Variation of temperature with heat source parameter
λ=0.001, α=π/3,A=0.25,Gr=5, F=0.1, Gm=5, M=0.5, Pr=1.5, Sc=0.2

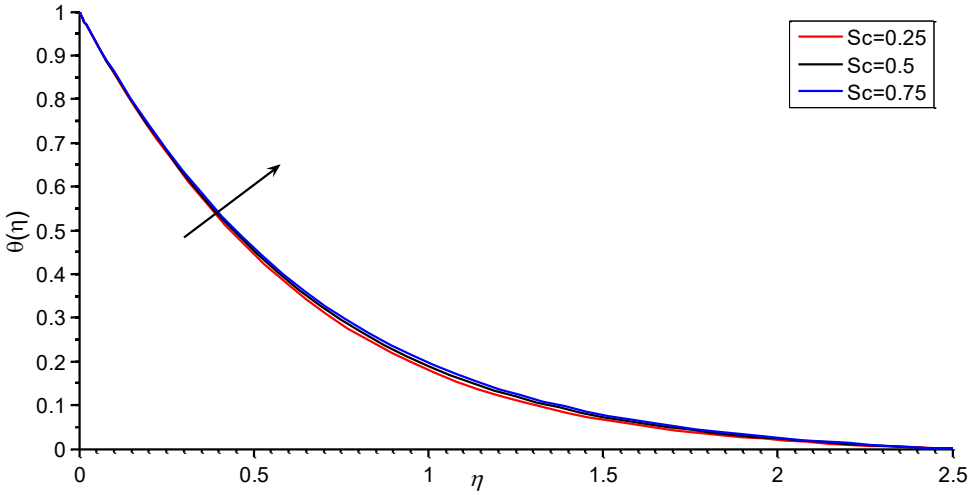

Figure7.19 Variation of temperature with heat source parameter
λ=0.001, α=π/3,A=0.25,Gr=5, F=0.1, Gm=5, M=0.5, Pr=1.5, Q=0.2

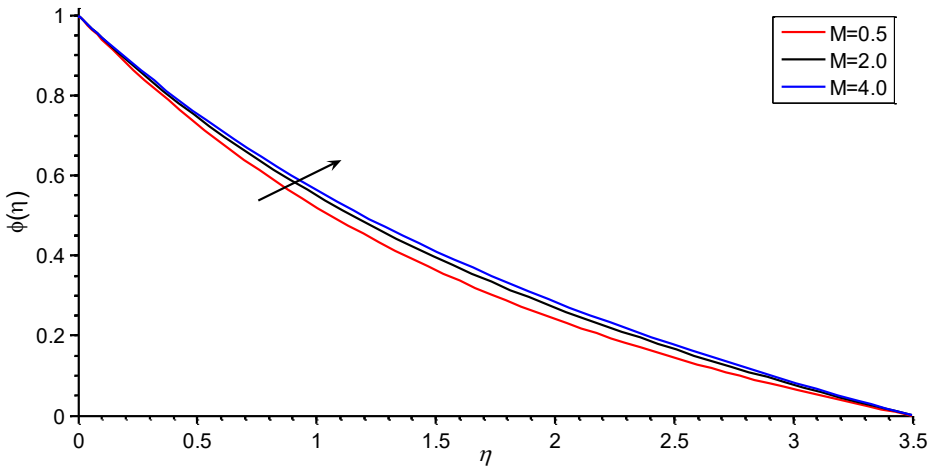

Figure7.20 Variation of concentration of fluid with the Hartmann number number
λ=0.001, α=π/3,A=0.25,Gr=5, F=0.1, Gm=5, Pr=1.5, Q=0.2, Sc=0.2

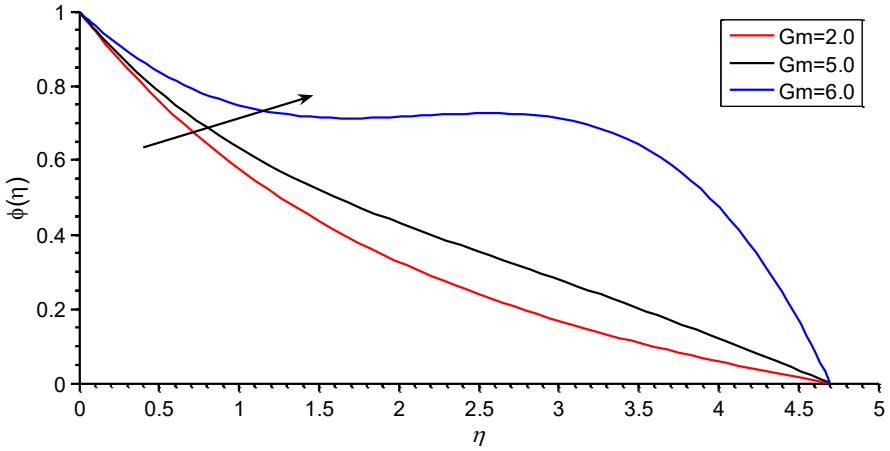

Figure7.21 Variation of concentration of fluid with the modified Grashof number
λ=0.001, α=π/3,A=0.25,M=0.5,Gr=2, F=0.1, Pr=1.5, Q=0.2, Sc=0.2

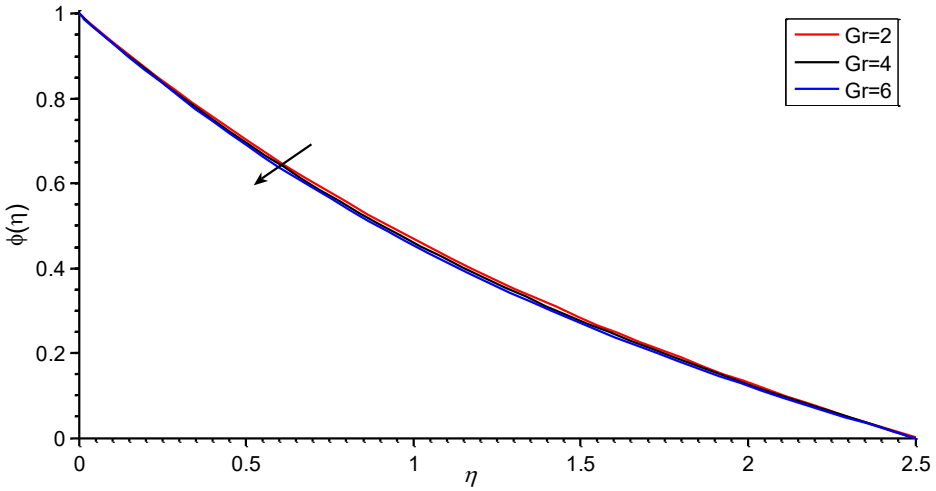

Figure7.22 Variation of concentration of fluid with the Grashof number
λ=0.001, α=π/3,A=0.25,M=0.5, F=0.2, Gm=5, Pr=1.5, Q=0.2, Sc=0.2

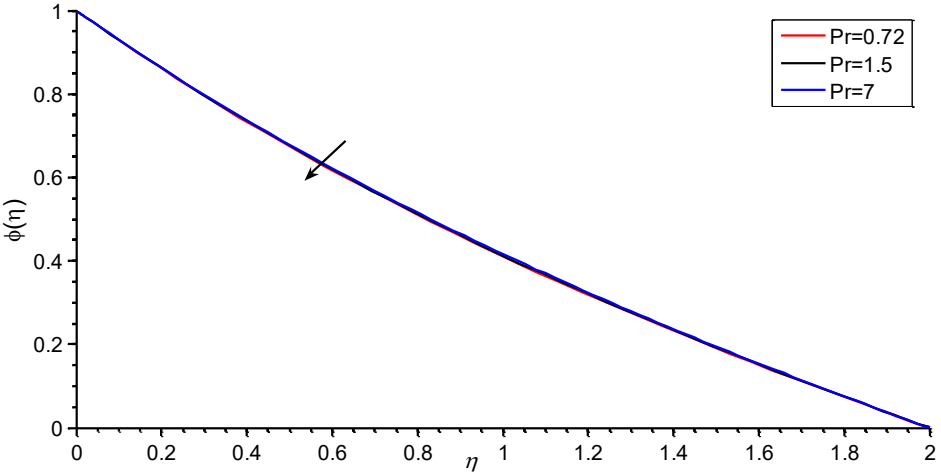

Figure7.23 Variation of concentration with the Prandtl number
λ=0.001, α=π/3,A=0.25,Gr=5, F=0.1, Gm=5, M=0.5, Q=0.2, Sc=0.2

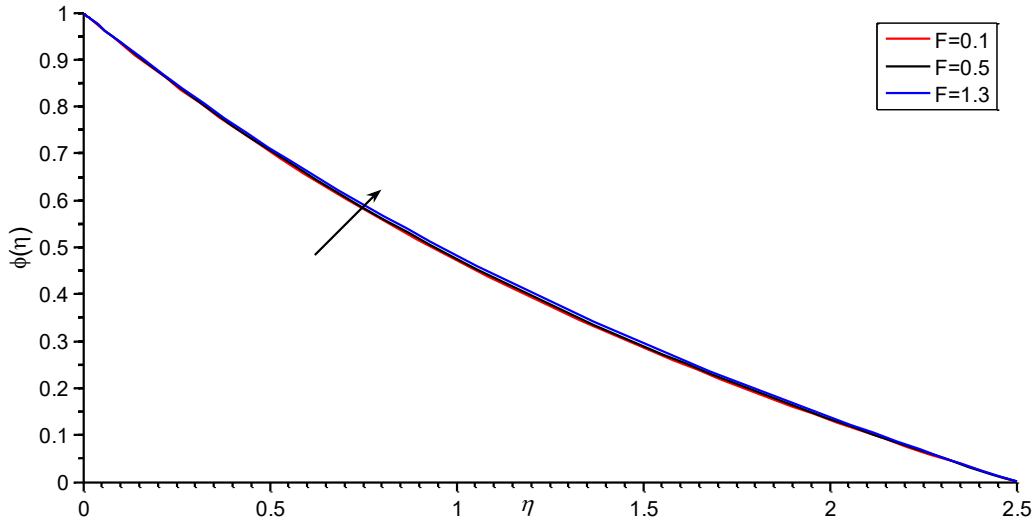

Figure7.24 Variation of cocentration of fluid with non-Darcy parameter at
α= π/3, λ=0.001, A=0.25, M=0.5, Gr=2, Gm=5, Pr=1.5, Q=0.2, Sc=0.2

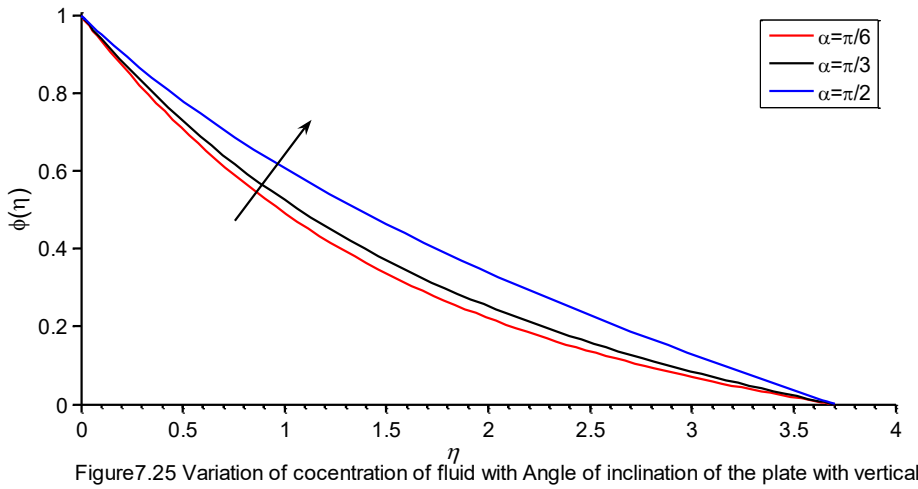

Figure7.25 Variation of cocentration of fluid with Angle of inclination of the plate with vertical
A=0.25 λ=0.001, M=0.5, Gr=2, Gm=5, Pr=1.5, Q=0.2, Sc=0.2

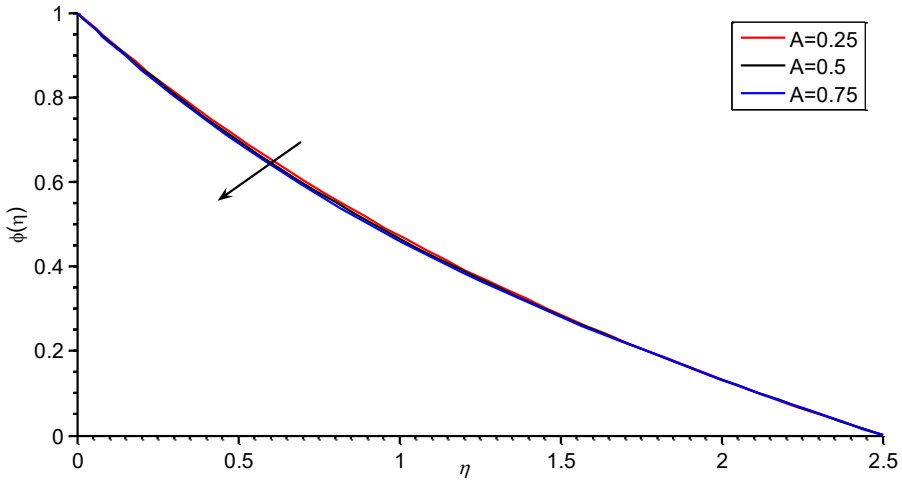

Figure7.26 Variation of cocentration of fluid with unsteadyness parameter at
α= π/3, λ=0.001, M=0.5, Gr=2, Gm=5, Pr=1.5, Q=0.2, Sc=0.2

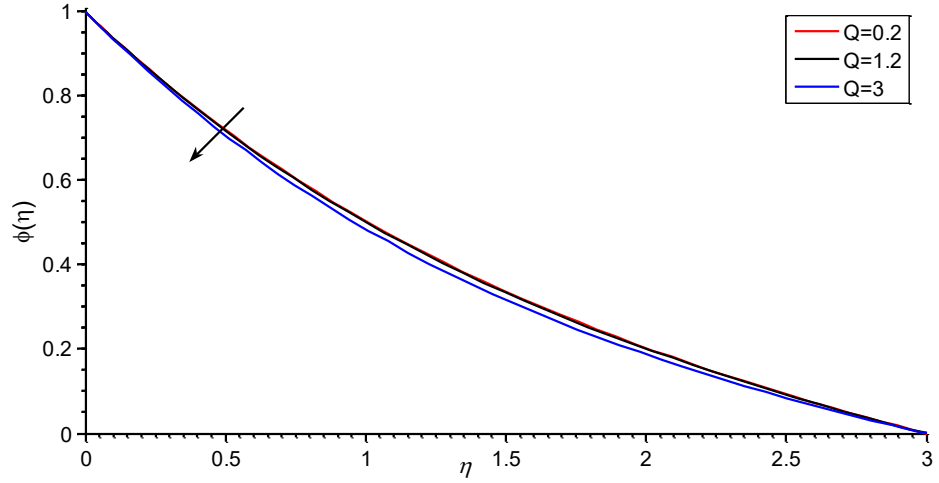

Figure7.27 Variation of concentration of fluid with heat source parameter
λ=0.001, α=π/3,A=0.25,Gr=5, F=0.1, Gm=5, M=0.5, Pr=1.5, Sc=0.2

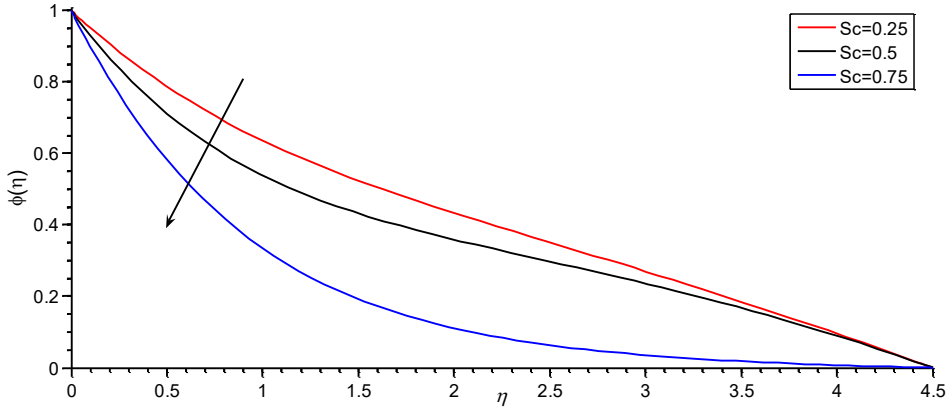

Figure7.28 Variation of concentration of fluid with Schmidt number
λ=0.001, α=π/3,A=0.25,Gr=5, F=0.1, Gm=5, M=0.5, Pr=1.5, Q=0.2